LBL-1503
UC-37 Instruments
TID-4500 (59th Ed.)

STIMULATED EMISSION IN NEON-HELIUM STREAMER CHAMBERS

Albert W. Stetz

November 1972

Prepared for the U. S. Atomic Energy Commission
under Contract W-7405-ENG-48

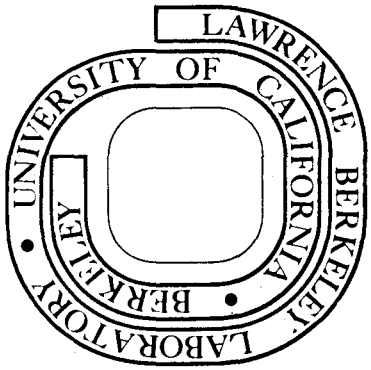

LBL-1503

DISCLAIMER

STIMULATED EMISSION IN NEON-HELIUM STREAMER CHAMBERS

Albert W. Stetz

Lawrence Berkeley Laboratory
University of California
Berkeley, California

ABSTRACT

We are investigating the possibility of using stimulated emission in the gas of a streamer chamber to improve the quality of the image that is photographed. The incremental gain from stimulated emission obtainable in a practical streamer chamber has been estimated from some related experiments with pulsed lasers. We have constructed a model of the dynamics of laser beam formation in a streamer chamber and estimated the light available for photography. Despite the uncertainties in these estimates, the calculations definitely suggest that a system in which the chamber is "primed" by an external light source would produce substantial gain in output light intensity compared with the conventional streamer chamber. We conclude with several suggestions for further research in streamer chamber improvements based on laser technology.

I. Introduction

There are striking similarities between the conventional streamer chamber and the pulsed neon-helium laser: The same gases are used and at roughly the same pressure, the same atomic transitions are employed and they are excited by comparable electric fields. There is an irresistible suggestion here to borrow some laser techniques in order to improve the streamer chamber in those areas where it is weakest, the luminosity and resolution of the particle tracks. This paper explores the possibility of using stimulated emission in the streamer chamber gas itself to improve the quality of the image which is photographed. We are encouraged at the start by the ease with which pulsed He-Ne lasers achieve enormous factors of gain in light intensity. In fact, most of the difficulties with gas lasers are specific to continuous operation and are of no consequence to a pulsed device. Moreover, our goals are modest. A heroic effort if required to build a conventional streamer chamber with marginally acceptable resolution; if we could manage a gain of ten in light intensity with stimulated emission this situation would change fundamentally--the streamer chamber would become a practical device. Finally, if there were light intensity to spare, one could open a new chapter in particle detection devices by building a variable pressure streamer chamber. The gas pressure in such a device would be adjustable for optimum ionization density measurements depending on the energy and the reactions one wished to observe. This information together

with the curvature of the tracks in a magnetic field could clarify many otherwise ambiguous reactions. The applications of the variable pressure streamer chamber to quark searches and to cosmic ray physics where momentum analysis is impracticable are as exciting as they are obvious.

The specific scheme which we investigate involves putting an ordinary streamer chamber in a Fabry -Perot cavity so that the discharge along the particle track forms the active medium of a pulsed neon-helium laser. The advantage of this arrangement is one of light collection efficiency. In a conventional streamer chamber installation the camera lens subtends about 10^{-5} to 10^{-6} of the total solid angle. A laser beam, on the other hand, is attenuated by about 10^{-2} by the semi-transparent mirrors but suffers no loss from solid angle. Thus if one could force as little as 1% of ordinary streamer light to originate from stiumlated emission, the effective light output of the chamber would be increased by at least an order of magnitude. The possibility of doing this depends on a number of parameters which have to be estimated from experience and theory of conventional lasers and streamer chambers.

The next section reviews the theory and experimental data pertinent to the design of Ne-He lasers. In the following sections we try to infer the incremental gain from stimulated emission obtainable in a practical streamer chamber from some experiments with pulsed lasers. Finally we construct a model of the dynamics of laser

beam formation in a streamer chamber and estimate the light available for photography. Our estimates are somewhat uncertain due to the difficulty in comparing the discharge conditions of the pulsed lasers to those in streamer chambers, but the calculations definitely suggest that a system in which the chamber is "primed" by an external source of laser light would produce substantial gain in output light intensity compared with the conventional streamer chamber at the cost of introducing a luminous background on which the streamers would appear. We conclude with several suggestions for further research in streamer chamber improvements based on laser technology.

II. Theory of Laser Operation[1]

A. Spontaneous and Induced Transitions

Consider the following simplified energy level diagram.

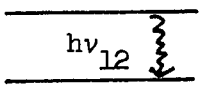

We imagine that E_1 and E_2 are excited states of an isolated atomic system such as a neon atom. Assuming that a radiative transition between these two states is not forbidden by the laws of quantum mechanics, there are three distinct ways this transition may occur:

a) Absorption

An atom in state E_1 absorbs a photon of energy $h\nu_{12}$ which leaves it in state E_2. Define the Einstein coefficient for absorption, B_{12}, by saying that W, the transition rate per unit time for this process, is given by

$$(1) \qquad W = B_{12} \int_0^\infty \rho(\nu)\, g_{12}(\nu)\, d\nu$$

where $\rho(\nu)$ is energy density per unit frequency interval of the photon flux, and $g_{12}(\nu)$ is the normalized line shape function for the transition, i.e. $g(\nu)\, d\nu$ is the probability that a given transition will result in the absorption or emission of a photon with energy between $h\nu$ and $h(\nu + d\nu)$. Of course

$$\int_0^\infty g(\nu)\, d\nu = 1.$$

Notice that W is a functional of ρ and g; e.g., if the frequency spectrum of the incident photon flux does not overlap the absorption spectrum then W = 0. B_{12}, however, is a true constant characteristic of the transition; its value must be determined experimentally. Unfortunately, there are several alternative definitions of B with different dimensionality in the literature. As it is defined here it carries the dimensions of volume/energy × time^2.

b) Stimulated Emission.

A system in state E_2 can absorb a photon of energy $h\nu_{12}$, and re-radiate it in coherence with another photon of the same energy leaving the system in state E_1. We can define the Einstein coefficient for stimulated emission, B_{21}, in the same way as that for absorption.

$$W = B_{21} \int \rho(\nu)\, g_{21}(\nu)\, d\nu \qquad (2)$$

Not surprisingly $g_{12} = g_{21}$. It can be shown, moreover, that $B_{12} = B_{21} \frac{m_2}{m_1}$ where m_i is the statistical weight or degeneracy of the ith state.

c) Spontaneous Emission

An atom in state E_2 can simply decay to state E_1 emitting a photon of energy $h\nu$ where ν is distributed about the central value ν_{12} according to the line shape function $g_{12}(\nu) = g_{21}(\nu) = g(\nu)$. The transition rate for spontaneous emission is simply equal to the Einstein coefficient $A_{21} = 1/\tau_{21}$, where τ_{21} is the mean lifetime for the system in state E_2 to decay to state E_1 in the

absence of external radiation. It can be shown[2] that the coefficients for induced and spontaneous emission are related by

$$(3) \qquad \frac{B_{21}}{A_{21}} = \frac{B_{12}}{A_{21}} \frac{m_1}{m_2} = \frac{c^3}{8\pi h\nu^3}$$

so that the rates of all three processes can be determined from a measurement of the lifetime for spontaneous decay.

As in all laser applications, we are interested primarily in stimulated emission. For this transition mode to predominate over absorption it is necessary to produce a population inversion between level E_1 and E_2, i.e. more atoms in state E_2 than in state E_1; otherwise photons from the $E_2 \rightarrow E_1$ transition would be absorbed faster than they were produced. This population inversion must be produced by some very specific non-equilibrium process, because the "natural" level population of thermodynamic equilibrium is proportional to $e^{-E_i/kT}$ where E_i is the energy of the i-th level, k is Boltzmann's constant and T is the temperature of the system. Moreover, it is increasingly difficult to maintain the population inversion against ordinary decay for shorter wavelength transitions. For example, imagine a flux of I monochromatic photons per square centimeter per second incident an atom in state E_2. The energy density

$$(4) \qquad \rho(\nu) = \frac{h\nu}{c} \delta(\nu - \nu_o) I.$$

The transition rate for stimulated emission is then

$$(5) \qquad W = \frac{\lambda^2}{8\pi\tau_{21}} g(\nu_o) I$$

where λ is the wavelength c/ν_o. In order for stimulated and spontaneous emission to be equally probable, the flux

$$(6) \qquad I = \frac{8\pi}{\lambda^2 g(\nu_o)} .$$

The λ^2 in the denominator makes short wavelength transitions impractical for laser operation. There are, in fact, very few usable transitions even in the visible region.

B. The Line Shape Function

Equation (6) also demonstrates the importance of the line width to stimulated emission, since $g(\nu_o)$ is rougly equal to $1/\Delta\nu$ where $\Delta\nu$ is the half-width of the spectral line. There are three separate mechanisms contributing to $\Delta\nu$ that need to be considered:

a) Natural Line Broadening

If an atom could be isolated and brought to rest, its transitions would be broadened only by the effect of the uncertainty principle and the finite lifetimes of its states. This produces a "Lorentzian" (or "Breit-Wigner" to the particle physicist) line shape given by

$$(7) \qquad g(\nu) = \frac{1}{\pi} \frac{\Delta\nu_n}{(\nu - \nu_{12})^2 + (\Delta\nu_n)^2} .$$

$\Delta\nu_n$ is the reciprocal of the effective radiative lifetime

$$(8) \qquad \Delta\nu_n = \frac{1}{2\pi} \left(\frac{1}{\tau_1} + \frac{1}{\tau_2} \right)$$

where τ_1 and τ_2 are the lifetimes of the initial and final states.

$$(9) \qquad \frac{1}{\tau_i} = \sum_j A_{ij}$$

where j ranges over all states to which state i can decay directly.

The natural line breadth is usually negligible compared with the doppler broadening due to the thermal motion of the atoms. For gases at low pressure (less than a few Torr) and near room temperature, the line shape is gaussian

$$(10) \qquad g(\nu) = \frac{1}{\Delta\nu_D}\sqrt{\frac{\ln 2}{\pi}}\ \exp\left[\frac{-(\ln 2)\,(\nu - \nu_{12})^2}{(\Delta\nu_D)^2}\right]$$

where $\Delta\nu_D$ is the Doppler half-width at half-power

$$(11) \qquad \Delta\nu_D = \nu_{12}\sqrt{\frac{2kT}{Mc^2}\ln 2}$$

with M the mass of the atom.

A third line broadening mechanism predominates at higher pressure. Each collision an excited atom suffers "sets its clock back to zero". This produces a Lorentzian line shape as given by (7) but with a $\Delta\nu_p$ derived from the mean lifetime between collisions rather than the natural lifetime of the state. $\Delta\nu_p$ is evidently proprotional to the gas pressure, but the constant of proportionality depends on the gas mixture and the atomic levels involved.[3]

C. Gain Relations for Lasers

Returning to Fig. 1, suppose there is a population density of n_1 atoms/cm^3 in state E_1 which is m_1-fold degenerate and n_2 atoms/cm^3 in the m_2-fold degenerate state E_2. An incident monochromatic flux of I photons per cm^2 per second will undergo a change dI in a distance dz given by

$$(12) \qquad dI = \frac{\lambda^2}{8\pi\tau_{21}}\, g(\nu_o)\, I\left(n_2 - n_1 \frac{m_2}{m_1}\right)\, dz.$$

The "gain" of a laser, G, is defined by

$$(13) \qquad G = \frac{1}{I}\frac{dI}{dz},$$

so

$$(14) \qquad G = \frac{\lambda^2}{8\pi\tau_{21}}\, g(\nu_o)\left(n_2 - n_1 \frac{m_2}{m_1}\right)$$

This is all, so far, well known. The task of determining the actual values of the parameters which appear in this equation for a given physical situation is not so clear cut. In the next sections we will try to estimate the lifetime, line width, and population density obtainable in a streamer chamber from some related experiments with neon-helium lasers.

III. Laser Transitions in Neon

A. Spectroscopy of Noble Gases

In order to describe the transitions that are important to the neon-helium laser and streamer chamber, we need to summarize some details of noble-gas spectroscopy.

Helium is something of an exception among the noble gases because it has no p-electrons and because it satisfies the L-S or Russell-Saunders coupling scheme quite well. The standard L-S notation is

$$n\,{}^{2S+1}L_J$$

where n is the principle quantum number of the excited electron, S is the total spin of the two electrons, J the total angular momentum, and L the total orbital angular momentum expressed as S,P,D,F, etc. The selection rules are

$$\Delta S = 0$$

$$\Delta L = 0, \pm 1$$

$$\Delta J = 0, \pm 1 \quad (0 \rightarrow 0 \text{ excluded})$$

Thus the lowest excited states of He, the 2^3S_1 followed by the 2^1S_0, are forbidden to decay to the $1S_0$ ground state by the ΔS and ΔJ rules respectively. Radiative cascades from higher energy states terminate on these metastables, which can be de-excited only by collisions.

The ground state of neon has six electrons in a closed p-shell. The total angular momentum J, the orbital angular momentum L, and the spin angular momentum of such a closed shell configuration

are all zero. When excitation takes place one of the electrons is promoted to an n' shell leaving a hole in the p shell. This hole behaves in many ways like a single p electron. It has spin = 1/2, ℓ = 1, and j = 3/2 or 1/2 with spin-orbit splitting (although of the opposite sign of a free electron). This hole couples with the promoted electron according to a scheme called Racah, or jℓ, or pair coupling. The orbital angular momentum of the outer electron ℓ' couples with the j of the hole to give a resultant K = j + ℓ', which is then coupled to the spin of the outer electron to give a total angular momentum J whose absolute value is K ± 1/2. The Racah labeling of the states consists of the symbol of the outer electron configuration followed by $[K]_J$. For example, the first excited states of neon are $3s[\frac{3}{2}]$ and $3s'[\frac{1}{2}]$. The prime on the s indicates that j of the hole was 1/2 rather than 3/2. The selection rules for jℓ coupling are

$$\Delta j = 0$$
$$\Delta K = 0 \pm 1 \quad (0 \rightarrow 0 \text{ excluded})$$
$$\Delta J = 0 \pm 1 \quad (0 \rightarrow 0 \text{ excluded})$$

The strongest lines satisfy the additional rule

$$\Delta J = \Delta K.$$

A list of the lowest excited states of neon is given in Ref. 1. At least as far as the energy levels are concerned the jℓ coupling scheme is very well satisfied. The energy differences between states of the same ℓ and j are consistently less than one percent of

the excitation energy. No matter how small the level splitting may be, however, it is enough to remove the $(2j + 1)(2\ell + 1)$-fold degeneracy one would expect from the coupling scheme alone. In other words, the m_i that appear in the transition rate equations are simply equal to $2J_i + 1$ where J_i is the total angular momentum of the ith state.

The lower-lying levels for neon are shown in Fig. 1 together with the metastable levels of helium. Most practical neon-helium lasers take advantage of the close coincidence between the helium metastables and the 4s and 5s neon levels to obtain population inversion by energy transfer in collisions of neon atoms in their ground state with excited helium atoms. The success of this scheme for obtaining inversion depends on two factors: the probability for energy transfer upon collision and the relative life-times of states between which the populations are to be inverted.

We will only consider the two strongest and best-studied lasing transitions in neon, the $5s' \left[\frac{1}{2}\right]_1 \rightarrow 3p' \left[\frac{3}{2}\right]_2$ transition at 0.6328μ and the $4s' \left[\frac{1}{2}\right]_1 \rightarrow 3p' \left[\frac{3}{2}\right]_2$ line at 1.1526μ in the near infrared. The first of these transitions is pumped by the 2^3S_1 level of helium and the second by the 2^1S_o state.

The de-excitation cross sections and the collision frequencies for He^*-Ne collisions have been measured and are listed in Table I

where Q is the collision cross section averaged over the thermal velocities of the atoms.

In considering the effect of transition rates on population inversion, it is necessary to distinquish between the lifetime of a state isolated from interactions with other atoms and the actual lifetime of an excited atom in a gas. The former is related to the strength of the transition or "oscillator strength" and is the lifetime which appears in place of the Einstein A coefficient in the rate equations. The actual lifetime is a function of pressure, temperature, and gas mixture and may be either longer or shorter than the theoretical lifetime due to the combined effects of inelastic collisions and resonance radiation trapping. It is this empirical "engineering data" which must be considered in deciding if population inversion is possible.

The lifetimes of the neon states involved in these transitions are listed in Table II. Clearly the conditions are ripe for inversion, but the task of calculating the actual degree of inversion obtainable for a given set of conditions, however, has proved to be very difficult. Various theoretical studies of population inversions in gas discharge systems have been attempted, but there is not enough detailed information available on inelastic scattering processes in the neon-helium mixture to permit getting much guidance from this type of calculation. We will try, instead, to infer the degree of population inversion obtainable in the streamer chamber discharge region from some related experimental parameters.

B. Laser Gain Parameters

Although the gain and population densities of continuous neon-helium lasers have been carefully measured and can be reliably predicted on the basis of laser geometry no comparable information exists for pulsed lasers. The difference lies in the fact that the population inversion in the continuous case is limited by the formation of the neon 3s metastable states. These states populate the 4p level by absorbing photons from $4p \rightarrow 3s$ transitions and thus destroy the inversion. The metastable states can be de-excited only by collision with the walls of the laser tube, so the gain and power output of a continuous laser depend on the tube diameter and gas pressure but beyond a certain level of excitation are almost independent of the discharge parameters. The importance of the metastables can be seen by comparing the typical power outputs of continuous lasers, say 10-100 milliwatts, with the 84 watts obtained from the pulsed Ne-He laser of Boot, Clunie, and Thorn.[6] We will try to use the results of this laser experiment to predict the gains obtainable in a streamer chamber discharge. The comparison involves some debatable theoretical assumptions, but is probably satisfactory for an order of magnitude estimate on the streamer chamber performance.

In the laser of Boot, Clunie, and Thorn a peak output power of 84 watts was obtained in a mixture of wavelengths including 1.118μ, 1.153μ, 1.162μ, and 1.206μ, all transitions of the $4s \rightarrow 3p$ group.

W. W. Rigrod[7] has developed a theory relating the power output of a 1.153μ laser to the gain and losses of the system. These results have been corroborated by a large number of measurements on lasers operating at low pressure (~ .8 Torr), and we will assume that they are still reliable in the high-pressure, high-gain region of the pulsed laser. We also assume that the Boot, Clunie, and Thorn laser is "pulsed" in the sense that the gain is not limited by the formation of metastables but "continuous" so far as Rigrod's formulation is concerned; that is, a quasi-equilibrium is reached between excitation and de-excitation mechanisms. This is plausible since the duration of the high voltage pulse (~ 1 μs.) is an order of magnitude longer than the mean life-times of the excited states and the photons in the cavity. Assuming that the linewidth is due only to collision broadening,

$$P = \tfrac{1}{2} A \omega_o t (\eta - 1) \tag{15}$$

where P is the total power output from one end of the laser, A is the area of the beam spot, t is the transmission fraction of the mirror, and η is the ratio of the unsaturated gain per pass to the total losses per pass, i.e.

$$\eta = \frac{g_o L}{a + t} \tag{16}$$

where a is the total loss per pass excluding transmission through the mirrors. The "saturation parameter" ω_o is a measure of the rate at which the population density is depleted by the laser beam.

Theoretically, it should be simply proportional to the total gas pressure so that we can scale up Rigrod's measurement at 0.8 Torr to the 245 Torr of the BCT laser. Neither the loss nor the transmission coefficients are reported by BCT, but typical operating values are a = .01 and t = .02. Collecting this information, we have

$$\omega_o = 1.8 \text{ watts/cm}^2$$

$$\eta = 222.$$

$$g_o = 1.48 \text{ cm}^{-1}$$

In the above calculations we have assumed that the BCT laser was a single-mode, single-frequency device; these are the conditions for which equation (15) was derived. In actual fact, a laser naturally oscillates at many discrete frequencies equally spaced at intervals of c/2L throughout the transition line. At each of these frequencies a laser may, in general, oscillate in several modes corresponding to various standing wave configurations within the tube. In conventional, low-pressure lasers multimode operation produces incredible complexity in the output spectrum. In high pressure lasers such as the BCT device, this complexity is completely washed out by the collision broadening. Each mode at each frequency depletes the population inversion over the entire linewidth and hence robs power from all other modes. As a consequence the total power from all modes within the line is equal to the power which would be contained in a single mode if all others could somehow be suppressed. This is the justification for using

equation (15) in the context of the BCT laser.

Since we will use this estimate for the gain in our estimates of streamer chamber performance, it is interesting to compare the discharge conditions in the pulsed laser with those in a streamer chamber. According to ref. 8 a visible streamer has roughly 10^{10} free electrons in a 1 m.m. region of space. If we take the electron drift velocity to be 2×10^7 cm/sec, the current density is

$$i = 10^{13}\ \text{cm}^{-3} \times 1.6 \times 10^{-19}\ \text{coulombs} \times 2 \times 10^7\ \text{cm/sec}$$
$$= 32\ \text{amps/cm}^2$$

The BCT laser had a peak current of 90 amps through a 2 cm diameter tube or 29 amps/cm^2 current density.

Finally, we can speculate as to what gain BCT would have measured if they had looked for the 6328 Å transition. According to the summary in table 5 - 11 in ref. 9 the gain of a continuous laser operating at 6328 Å is about one-fifth of that of a comparable laser operating at 1.152μ. Consequently we would expect a gain of roughly 0.3 cm^{-1}.

The population inversion density corresponding to these gains can be calculated from equation (14) if $\Delta\nu_p$ is known. Unfortunately, the collision broadening has not been measured for the 1.152 μ transition except at very low pressure. P. W. Smith[10] has measured $\Delta\nu_p$ for the 6328 Å transition at pressures up to 4 Torr, however, and it is probably good enough to extrapolate his measurement up to 245 Torr to evaluate the BCT device (and later to atmospheric pressure to determine streamer chamber performance). The results are summarized in table III. These inversion density results should be compared with the ionization density estimates for streamers in ref. 8 It is suggested in this work that there are "at least" 10^{10} ion pairs per streamer (or 10^{13} pairs per cm^3) and that the ratio of the number of visible photons produced in the discharge to the number of ion pairs is roughly equal to one. This would be consistent with table IV if most of the visible light came from the 6328 Å transition. Spectrographs of actual streamer chamber spectra,[11] however, show a large number of visible lines including most of the 5s → 3p and 3p → 3s transitions. There are several possible reasons for this discrepancy:

1. Lasers commonly operate with a mixture of 90% He to 10% Ne to enhance the pumping of the 5 s' [$\frac{1}{2}$] state, whereas most streamer chambers (for no particular reason) use 10% He and 90% Ne so that the optical transitions are excited more uniformly.

2. As the result of a collision, the excitation of a specific level can be transferred to another state in the same multiplet. The

result of this "cross-population" is to spread the output power of the laser over a number of closely spaced transitions all originating and terminating in the same multiplets.

3. Although the peak ionization densities in the BCT laser and the streamer chamber discharge are presumably comparable, the effective inversion densities may not be because of the longer high voltage pulse in the BCT experiment.

Finally, we can make a general argument based on the selection rules that at most 10% of all visible light comes from $5s \rightarrow 3p$ transitions. Evidently

	number of photons from $4s \rightarrow 3p$ transitions	(visible)
+	number of photons from $5s \rightarrow 3p$ transitions	(infrared)
$\approx$	number of photons from $3p \rightarrow 3s$ transitions	(visible)

We have ignored all mechanisms of populating the 3p states except for decay from higher states. Faust and McFarlane[12] have calculated relative line strengths for the $s \rightarrow p$ transitions in neon and compared them with measured values of the gain parameter. Their numbers suggest that the maximum obtainable population density for the 5s states is about ten times that of the 4s states, but whereas the 4s states all decay to 3p, the 5s decays preferentially to 4p (a useless far infrared transition) with a branching ratio

$$\frac{\text{Rate } [\ 5s \rightarrow 4p\ ]}{\text{Rate } [\ 5s \rightarrow 3p\ ]} \approx 100$$

We conclude that at most 10% of the visible light from a Ne - He discharge results from 5s → 3p transitions. Furthermore, the number of 4s → 3p photons is roughly equal to the total number of visible photons.

Further speculation on the mysteries of gas discharges on the basis of so little data is probably quite futile. One is left with the impression that the gains and inversion densities listed in table III may be unrealistically large. Since, as will be seen in the next section, the light amplification of the laser-streamer chamber depends exponentially on the gain, it is impossible to determine how well the device will work without specific measurements of the gain obtainable in the streamer chamber discharge.

IV. Stimulated Emission in Streamer Chambers

Imagine a streamer chamber placed between mirrors so that the discharge in the chamber constitutes the active volume of a "laser". The arrangement is shown schematically in Figure 2. The spherical-confocal mirrors eliminate the need for any further focusing of the light, and their alignment is much less critical than the alignment of flat mirrors. In order to estimate how much light will be available for photography outside of the mirror system we must take into account the interaction of stimulated emission, spontaneous decay, and absorption of light in the cavity. Our starting point will be a pair of coupled first-order differential equations for the time-behavior of the population inversion and the flux of photons in the cavity.

We denote the inversion density $n_2 - n_1 \frac{m_2}{m_1}$ appearing in equations (12) and (14) by N. Assume that a population inversion N_o is created at time $\tau = 0$ by the pulsing of the streamer chamber. This density will decline to zero after some period of time due to spontaneous and stimulated emission. (To a good approximation, n_1 is identically zero because of the fast $3p \rightarrow 3s$ transition.) We will assume that the photon flux in the medium is small enough that essentially all the states are de-excited spontaneously. (We should be so fortunate as to be wrong!) Then

$$\frac{dN}{d\tau} = -\frac{N}{\tau_2} , \tag{15}$$

where τ_2 is the actual lifetime of the upper state in the streamer chamber.

The photon flux I in the laser beam originating from a streamer in the chamber[13] contains both stimulated as well as spontaneously emitted photons. This flux is attenuated in the cavity by a combination of absorption, diffraction, and transmission through the mirrors. These effects combine to form a mean photon lifetime τ_{phot}. In other words,

$$\frac{dI}{d\tau} = -\frac{I}{\tau_{phot}} + \frac{VN\Omega}{\tau_2} + \frac{c\ G_o\ \beta\ N\ I}{N_o} \tag{16}$$

where VN is the total inverted population contained in the streamer volume and Ω is the fraction of solid angle subtended by the laser beam. G_o is the initial gain per unit length and β is the ratio of the length of the streamer to the distance between the mirrors. Eliminating τ by combining (15) and (16) yields

$$\frac{dI}{dn} = \frac{\tau_2}{\tau_{phot}} \quad \frac{I}{n} - VN_o\Omega - G_o\ c\ \beta\ \tau_2\ I \tag{17}$$

where

$$n = N/N_o$$

In order to simplify the notation we identify the dimensionless coefficients

(18) $$C_S = V N_o \Omega$$

$$C_D = G_o c \beta \tau_2$$

$$C_B = \tau_2 / \tau_{phot}$$

the starting, driving, and braking terms respectively. Then equation (17) becomes

(19) $$\frac{dI}{dn} = C_B \frac{I}{n} - C_S - C_D I$$

This can be integrated using standard techniques, although we can expect trouble at n = 0. A self-starting laser-streamer chamber corresponds to the boundary condition

(20) $$I (n = 1) = 0$$

The solution to (19) satisfying (20) is

(21) $$I (n) = C_S n^{C_B} e^{-C_D n} \int_n^1 x^{-C_B} e^{C_D x} dx$$

We are really only interested in the total light integrated over all time.

(22) $$T = \int_o^x I(t)dt = \int_o^1 I(n) \frac{dn}{n}$$

$$= C_S \int_o^1 n^{C_B - 1} e^{-C_D n} dn \int_n^1 x^{-C_B} e^{C_D x} dx$$

The integrals must be evaluated numerically; however, it is easy to prove that they converge. Obviously

$$T < C_S e^{C_D} \int_0^1 dn\, n^{C_B - 1} \int_n^1 x^{-C_B} dx$$

but now the integrals can be done in closed form, and in fact are well behaved.

From the point of view of numerical integration it is convenient to integrate (22) once by parts so that

$$T = \frac{C_S}{C_B} + \frac{C_S C_D}{C_B} f(C_B, C_D) \tag{23}$$

where

$$f = \int_0^1 dn \int_n^1 dx \left(\frac{n}{x}\right)^{C_B} e^{C_D (x - n)}$$

The advantage of equation (23) over (22) lies in the fact that the integrand is bounded and that f is a slowly varying function of the coefficients. f is graphed as a function of C_B and C_D in figure 3.

The data given in the previous sections can be used to estimate the coefficients. If we assume the values of the loss parameters used in section III then the photon lifetime is

$$\tau_{phot} = \frac{L}{c(a+t)} \approx 50 \text{ ns.}$$

for 50 cm mirror spacing. C_B is therefore on the order of unity depending on the transition and the exact construction of the streamer chamber. If $\beta = .005$ (2.5 mm streamer length), $C_D = 22.5$ for the 1.15 μ transition and 4.5 for the 6328 Å transition. The solid angle of the laser beam would be zero if it were not for diffraction in the cavity which produces a small angular divergence. Boyd and Gordon[14] have shown that the half-width $\delta\theta$ between half-power points for confocal mirror geometry occurs at

$$\delta\theta = \frac{\ell n 2}{\pi}\sqrt{\frac{\lambda}{L}}$$

The fractional solid angle, $\frac{1}{2}\delta\theta^2$, is 1.4×10^{-7} for the shorter wave length and 2.6×10^{-7} for the longer.

There is one more factor to be estimated which does not appear in equation (22). The I which appears here is really the light flux from a single mode operating at the center of the line. The useful light output from the device is equal to I times the transmission coefficient times the effective number of modes participating. Since the modes are separated by a frequency interval of c/2L the effective number of them is approximately

$$\frac{2L}{c}\,\pi\,\Delta\nu = 600$$

The important parameters and the final light output are summarized in table IV. For purposes of comparison, about 10^3 photons are required to expose one 7-micron grain of film and at least 10 to

100 grains must be exposed if the streamer is to be photographically detectable. Evidently the light output from the visible transition of our hypothetical laser-streamer chamber compares unfavorably with the unaided streamer chamber, but the light from the infrared transition, if it could be photographed with reasonable sensitivity, would be enormously amplified. This large difference in light output can be traced to the rather small difference between the G_o's, which enter in equation[22] as exponents. Since our estimates of the gain attainable in a streamer chamber could easily be wrong by a factor of five in either direction one is left with the impression that the self-starting laser-streamer chamber might work but that one should first look at other schemes.

One obvious way to try to improve on the previous scheme is to prime the chamber with an external light source. In this way the small fractional solid angle factor in C_S is avoided at the cost of introducing a luminous background on which the streamers must appear. In other words, we trade an intensity problem for a signal to noise problem. We can easily calculate the signal to noise ratio, however, with the odds and ends which have already been collected.

We can conceptualize the priming operation as follows: at some time prior to the pulsing of the streamer chamber a neon-helium laser light source is turned on so that the active volume of the streamer chamber is illuminated with a uniform light flux of I_o photons per square centimeter per second. In the absence of any amplification

these photons will be partially trapped in the chamber where they will decay with their characteristic lifetime. The time dependence of the trapped light satisfies

$$\frac{dI}{dt} = \frac{I_o}{(\frac{2L}{c})} - \frac{I}{\tau_{phot}} \tag{24}$$

and the steady-state solution is

$$I = I_o \frac{(c\ \tau_{phot})}{2L} \tag{25}$$

Imagine now that when the chamber is pulsed a fast camera shutter (a Kerr cell, for example) is opened and closed a time T thereafter. During this interval the camera will receive a total flux of $I_o \frac{(c\ \tau_{phot})}{2L}$ tT photons per square centimeter from those regions of the chamber where there is no discharge. (t is the mirror transmissivity). The active areas of the chamber will emit light according to an equation much like (16)

$$\frac{dI}{d\tau} = \frac{-I}{\tau_{phot}} + \frac{I_o\ c}{2L} + \frac{c\ G_o\ \beta\ N\ I}{N_o} \tag{26}$$

simplifying as before we get

$$\frac{dI}{dn} = C_B \frac{I}{n} - C_p \frac{1}{n} - C_D\ I \tag{27}$$

where $c_p = \tau_2 I_o c/2L$. The boundary condition is

$$(28) \qquad I(n = 1) = I_o \left(\frac{c\,\tau_{phot}}{2L} \right) = \frac{C_p}{C_B}$$

and the solution is

$$I = C_p\, n^{C_B} e^{-C_D n} \int_n^1 x^{-C_B-1} e^{C_D x}\, dx +$$

$$(29) \qquad + \frac{C_p}{C_B}\, n^{C_B} e^{-C_D (n-1)}$$

The signal to noise ratio or the relative brightness of the streamer on the illuminated background as seen by the camera during the interval T is

$$(30) \qquad \frac{S}{N} = \int_o^T dt I(t) \Big/ \frac{C_p\, T}{C_B}$$

Naturally one chooses T so as to maximize equation (30). The maximum attainable S/N and the required time interval are plotted in Fig. 5. Notice that S/N is independent of I_o and independent of t except as it appears in C_B. Therefore, one can further optimize the chamber performance by making the mirror transmissivity as small as possible and then adjusting I_o so that the brightness of the image is optimum for the film. The only limitation on I_o is imposed by the initial assumption that essentially all the states decay spontaneously, but this is not an important restriction so far as ordinary photography is concerned.

A glance at Fig. 4 shows that signal-to-noise ratio for the visible transition is marginal, whereas the infrared transition is overwhelmingly bright. This again reflects the small differences in the values of C_D for the two transitions, and again it must be pointed out that the margin between success and failure is much smaller than the uncertainties in our estimates of the gains.

V. Conclusion

We have explored several schemes for using stimulated emission to increase the amount of photographable light from a neon-helium streamer chamber. The estimates of the performance of these devices suggest that unless one is willing to use infrared photography, the laser-streamer chamber techniques can at best equal the performance of an ordinary streamer chamber. This is hardly a recommendation for undertaking such a project, especially in view of the difficulty in building and aligning large, curved, semitransparent mirrors. Our investigations, however, do suggest several interesting lines for further research:

1. The performance of the laser-streamer chamber depends sensitively on the differential gain obtainable in the streamer chamber discharges. Since our estimate of this parameter is not very accurate it should be measured experimentally. An increase of a factor of five over the calculated gain would make the scheme quite practical.
2. There may be considerable advantage in using infrared photography both for the conventional and the laser-amplified streamer chamber. Neon simply has many stronger lines in the 1-micron range than in the visible spectrum.

3. The strength of the visible transitions might be enhanced by optimizing the gas mixture. If experience with continuous lasers is a reliable indication, increasing the ratio of helium to neon should make ordinary streamers much brighter.

Finally, there are some far-fetched, laser-oriented ideas which come to mind, such as resonance scattering of laser light from the streamers or laser induced ionization along the path of the ionizing particle.[15] Whether or not any of these particular schemes actually turns out to be practical, the laser and the streamer chamber are such closely related devices it is hard to imagine that their marriage will not bear fruit.

Table I

Collision	Q ($\times 10^{-16}$ cm^2)	Collision frequency, per metastable/sec p in mm. Hg
$He(2^1S_o) \rightarrow Ne(4s')$	4.1 ± 1	$17 \times 10^5 P_{Ne}$ [4]
$He(2^3S_1) \rightarrow Ne(5s')$	0.37 ± 0.05	$1.6 \times 10^5 P_{Ne}$ [5]

Table II

Transition	State	Total Radiative Lifetime	Ref.	Transition Lifetime	Ref.
1.1526	$4s'[\frac{1}{2}]_1$	96 ns	c.	229 ns	a.
	$3p'[\frac{3}{2}]_2$	12 ns	d.		
0.6328	$5s'[\frac{1}{2}]_1$	--	b.	723 ns	a.
	$3p'[\frac{3}{2}]_2$	12 ns	d.		

a) Result of theoretical calculation by W. L. Faust and R. A. McFarlane, Journal of Applied Physics 35, 2010 (1964).

b) This lifetime has not been measured due to the difficulty of disentangling the decay time from the $3p \rightarrow 3s$ spectra. Presumably it is comparable to the $4s'[\frac{1}{2}]_1$ lifetime.

c) Measured directly by observing decay time after electron excitation. W. R. Bennett, Advances in Quantum Electronics, ed. Singer, Columbia Press (1961).

d) Measured by negative dispersion technique by Landenburg, Rev. of Mod. Phys. 5, 243 (1933).

TABLE III

Calculated Gain and Inversion Density for Pulsed Ne-He Discharge

Transition	$\Delta\nu_p$ 245 Torr	$\Delta\nu_p$ 760 Torr	G_o	N
1.153 μ	1.9×10^{10} sec^{-1}	5.8×10^{10} sec^{-1}	1.5	3.8×10^{13} cm^{-3}
.6328 μ	1.9×10^{10} sec^{-1}	5.8×10^{10} sec^{-1}	.3	8.1×10^{13} cm^{-3}

TABLE IV

Parameters for the Self-Starting Laser-Streamer Chamber

Mirror Spacing	L = 50 cm.
Mirror transmission coefficient	t = 0.02
Fractional loss per pass	a = 0.01
Streamer length	2.5 mm.
Streamer cross-sectional area	1 mm^2
Photon lifetime	τ_{phot} = 50 ns.
Upper level Lifetime	τ_2 = 96 ns.

Transition	C_B	C_D	C_S	f	Photons
1.152 μ	1.9	22.5	2.5×10^4	9.8×10^4	3.5×10^{11}
0.6328 μ	1.9	4.5	2.8×10^4	0.5	5.7×10^5

Notes and References

1. Most of this material can be found in the standard references; for example, W. V. Smith and P. P. Sarokin, The Laser, McGraw-Hill, New York, 1966; H. G. Heard, Laser Parameter Measurements Handbook, John Wiley & Sons, New York, 1968; D. C. Sinclair, W. E. Bell, Gas Laser Technology, Holt, Rinehart and Winston, New York, 1969.

2. This result was first obtained by Einstein, Phys. Z., 18:121 (1917) on the basis of a simple thermodynamic argument. For a (slightly) more up to date derivation see W. Heitler, The Quantum Theory of Radiation, Clarenden Press, Oxford, 1954. Stimulated emission comes from the "disconnected" forward scattering part of the scattering amplitude, hence the surprising result that the ratio of an amplitude with one external photon line to an amplitude with three external photons should be independent of the coupling constant!

3. An awesome body of theory exists on this subject. See, for example, R. G. Breene, Jr., The Shift and Shape of Spectral Lines, PerGamon Press, New York, 1961.

4. E. E. Benton and W. W. Robertson, Bull. Am. Phys. Soc., 7:114 (1962).

5. A. Javan, W. R. Bennett, Jr., and D. R. Herriott, Phys. Rev. Letters, 6:106 (1961).

6. H. A. H. Boat, D. M. Clunie, and R. S. A. Thorn, Nature, 198:773 (1963).

7. W. W. Rigrod, Journal of App. Phys., 34:2602 (1963).

8. F. Bulos, A. Odian, F. Villa, and D. Young, SLAC Report No. 74, 1967.

9. Smith, Sorokin, op. cit.

10. P. W. Smith, I.E.E.E. Journal of Quantum Electronics, Vol. QE-2, No. 4 (1966).

11. I am indebted to N. Anderson, Lawrence Berkeley Laboratory, for showing me his spectrographs taken at the SLAC 2-meter streamer chamber. Qualitatively, the streamer chamber spectrum resembles the Neon glow discharge spectra as listed, for example, in Handbook of Chemistry and Physics, 40th ed., Chemical Rubber Publishing Co., Cleveland, 1958, pp. 2829-2932.

12. W. L. Faust and R. A. McFarlane, Journal of Applied Physics, 35:2010 (1964).

13. In this section (only) I has the dimensionality of photons per second per streamer rather than photons per second per square centimeter.

14. G. D. Boyd and J. P. Gordon, Bell System Tech. Journal, 40:489 (1961).

15. E. Gygi and F. Schneider, CERN/ISR-GS/69-46 (1969).

FIGURE CAPTIONS

1. The lower-lying levels of neon together with the metastable levels of helium.

2. Schematic drawing of the laser-streamer chamber.

3. Plot of the function F for various chamber parameters.

4. Signal to noise ratio and optimum image formation time for various chamber parameters.

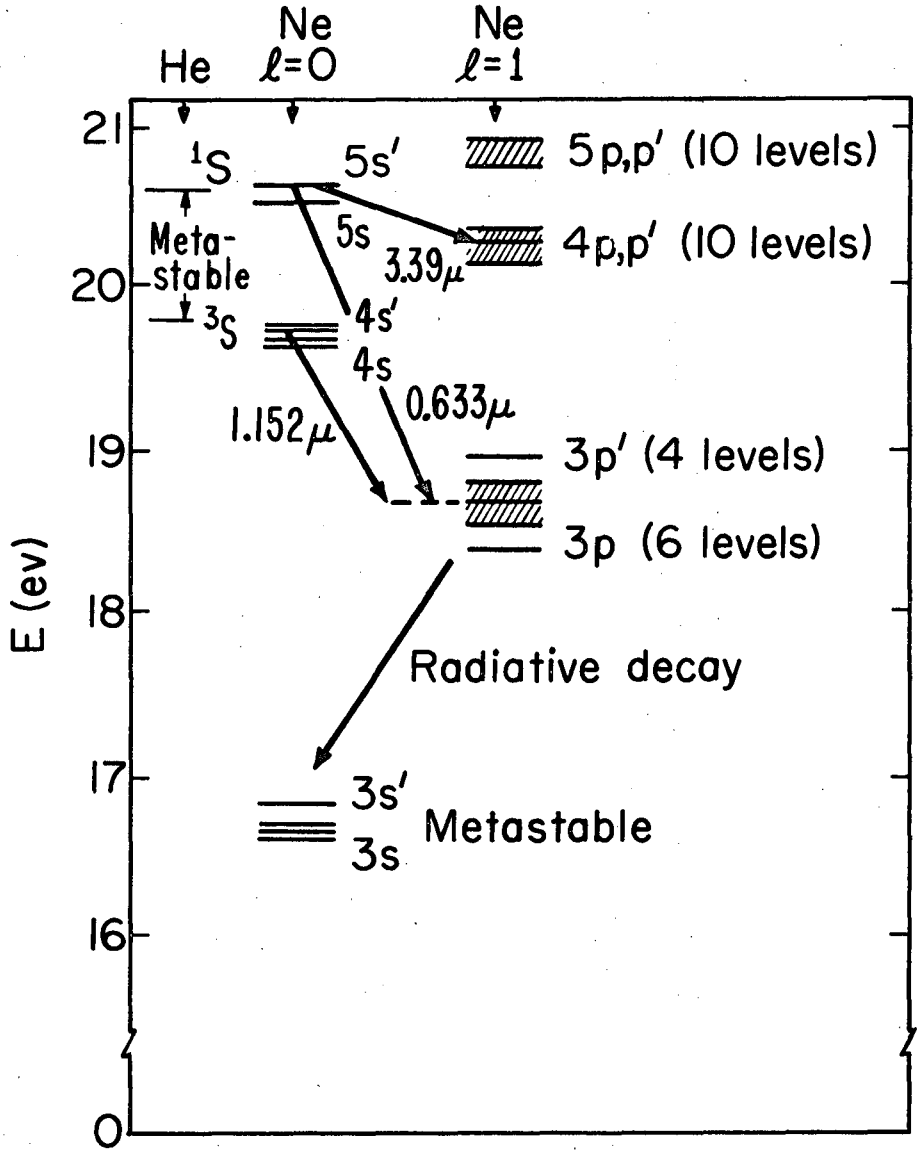

XBL726-3287

Fig. 1

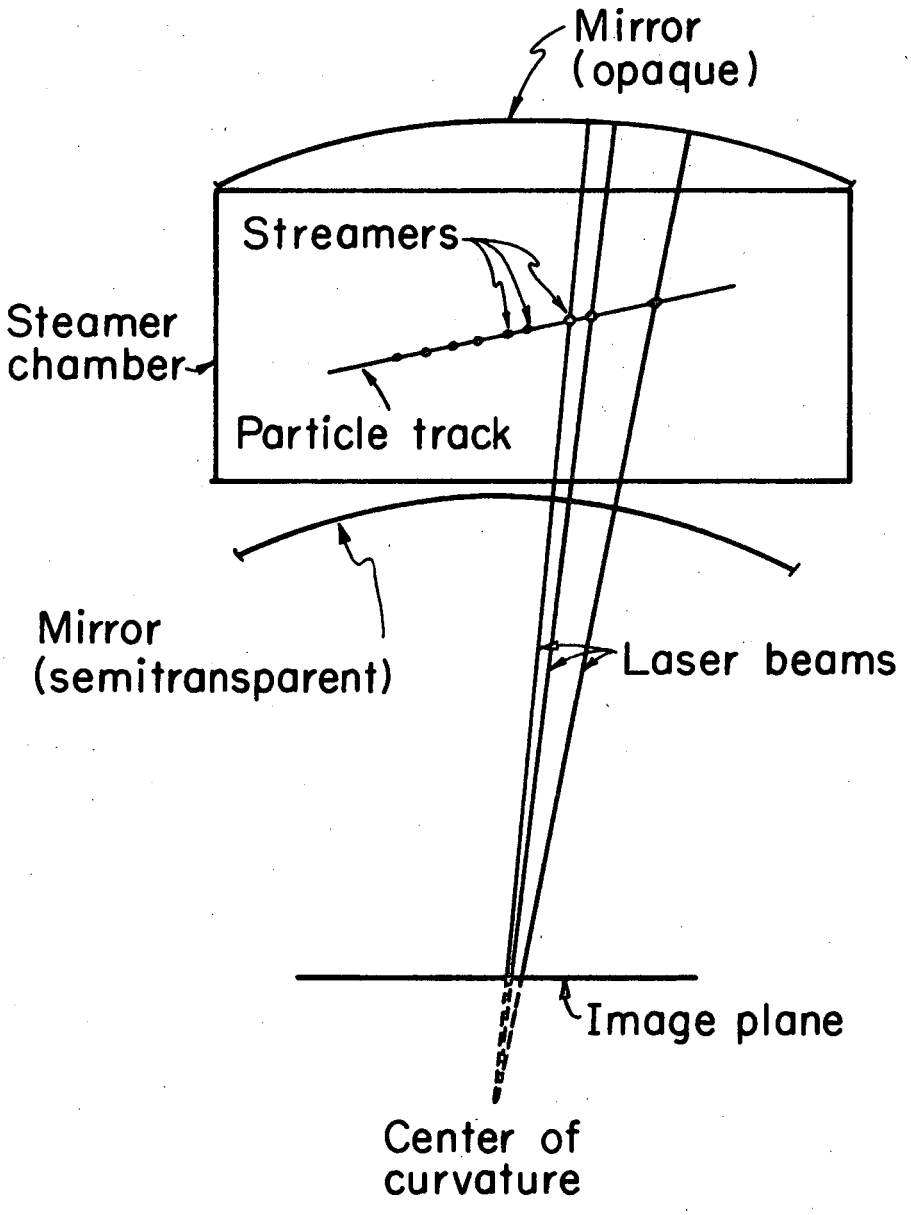

XBL726-3290

Fig. 2

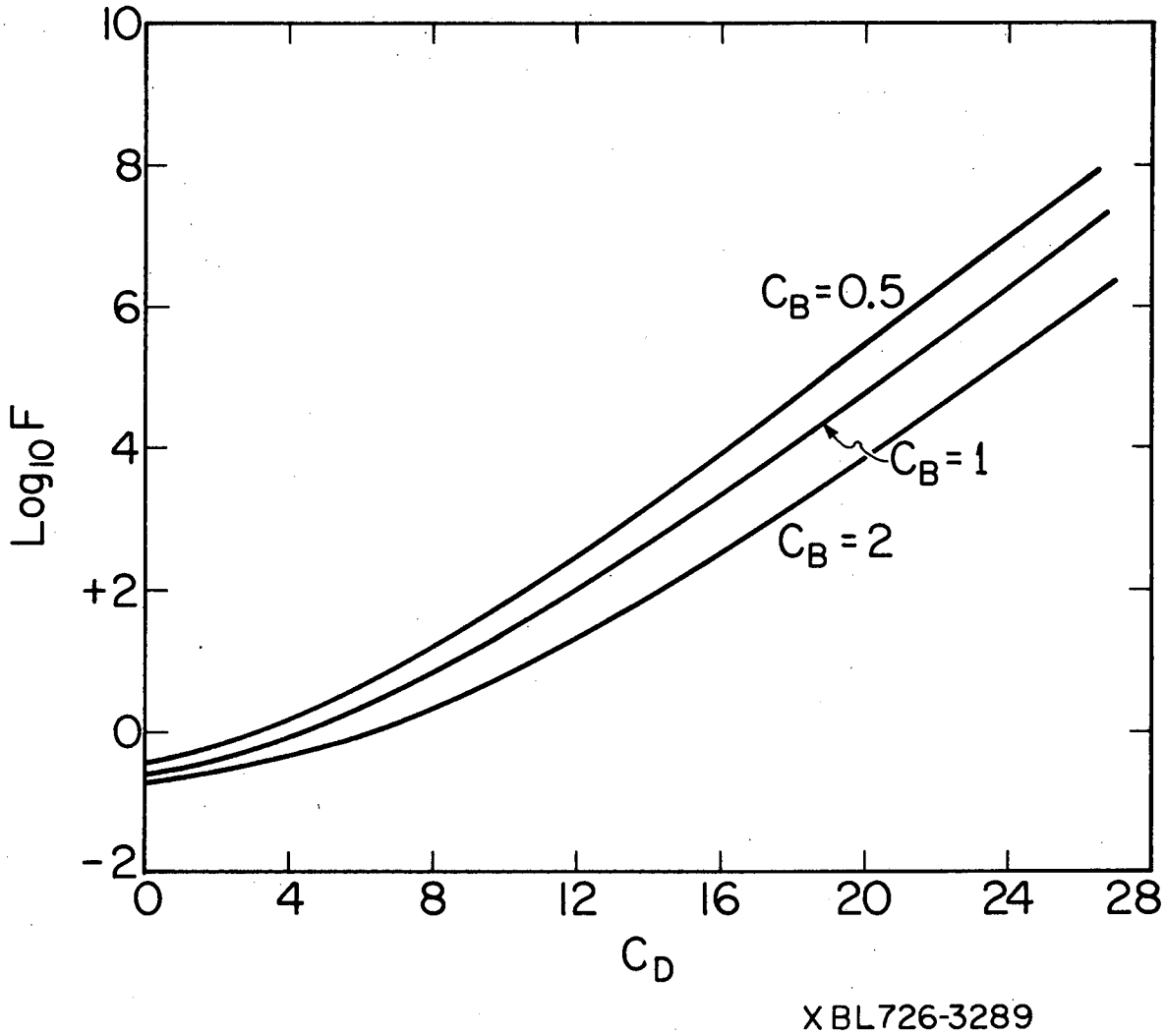

Fig. 3

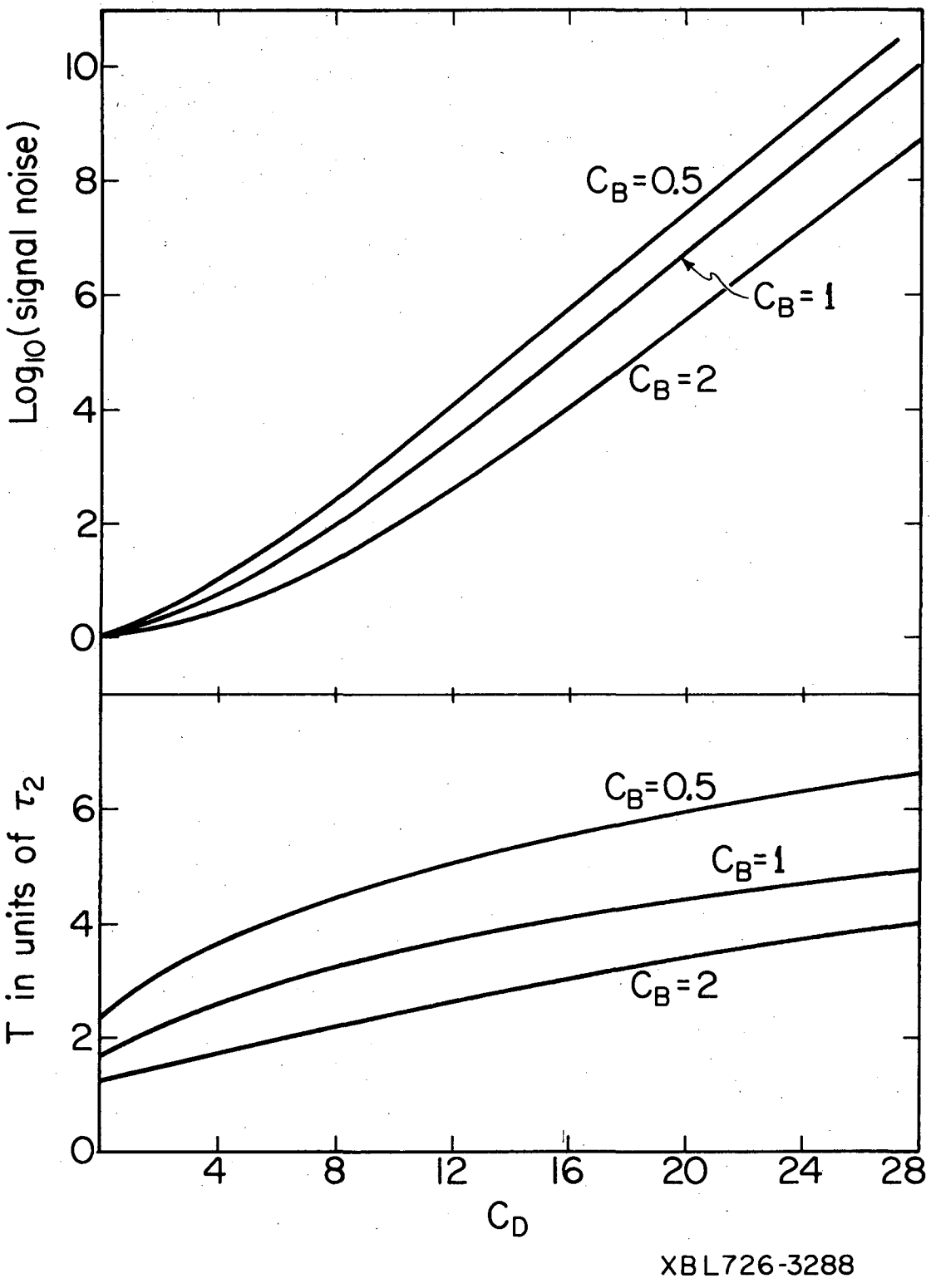
Log10(signal noise)
10
8
6
4
2
0
CB=0.5
CB=1
CB=2
T in units of τ2
6
4
2
0
CB=0.5
CB=1
CB=2
4
8
12
16
20
24
28
CD
XBL726-3288

Fig. 4

TECHNICAL INFORMATION DIVISION
LAWRENCE BERKELEY LABORATORY
UNIVERSITY OF CALIFORNIA
BERKELEY, CALIFORNIA 94720